

STUDY OF PION-PION RESONANCES IN 3.3-BeV $\pi^- - p$ INTERACTIONS*

Zaven G. T. Guiragossian†

Lawrence Radiation Laboratory, University of California, Berkeley, California

(Received 9 May 1963)

We have studied the interactions

$$\pi^- + p \rightarrow \pi^- + \pi^+ + n \quad (a)$$

and

$$\pi^- + p \rightarrow \pi^- + \pi^0 + p \quad (b)$$

in the Lawrence Radiation Laboratory 72-in. hydrogen bubble chamber exposed to a (3.3 ± 0.1) -BeV/c π^- beam from the Bevatron. The beam momentum and uncertainty were determined by the measured momentum distribution of incoming tracks of length greater than 60 cm and proper entrance angles.

Data reduction was performed with the FOG-CLOUDY-FAIR system. With the above beam momentum and uncertainty, two-prong events were fitted to reaction types (a) and (b). Events with proper beam acceptance angles, converging iterations, and χ^2 values ≤ 5.5 for either reaction were examined. Separation into Reaction (a) or (b) was done by determining the ionization and range of the positively charged tracks, up to 1.0-BeV/c momenta. The missing neutral masses were computed for both types by using measured parameter values. For the separated events, the distribution of missing mass squares of (a) gave a peak at the neutron mass and another near the $(n + \pi^0)$ mass. For (b), we obtained a peak at the π^0 mass, and enhancement at the η mass. The missing mass squares were computed by $M_0^2 = (E_{\pi^-} - M_p - E_{\pi^+} - E_{\pi^0})^2 - (P_{\pi^-} - P_{\pi^+} - P_{\pi^0})^2$. Cuts were then imposed to define the desired neutral masses for the entire sample. Further, a "good-measurement" criterion was applied to the entire data. Including 1700 elastic interactions a total of 5000 two-prong events were measured. Thus, 532 events were identified as Reaction (a) and 365 events as Reaction (b); these include 30 half-weighted ambiguous events which had high momentum transfers to the nucleon.

Experimental results. — We have computed the "dipion" effective mass, ω ; the invariant momentum transfer to the nucleon, $t = \Delta^2/\mu^2$; and the angle between the incoming and outgoing π^- in the barycentric system of the final pions, $\Theta_{\pi\pi}$. The beam momentum uncertainty contributed approximately 15 MeV to the error in ω , and other errors brought this to about 35 MeV; accordingly,

we chose to make a histogram of ω in 50-MeV intervals. Figures 1(a) and 1(b) show the histogram of the "dipion" mass for the $(\pi^-\pi^+)$ and $(\pi^-\pi^0)$ states, respectively. The (π^-, π^0) spectrum is strongly peaked at $\omega_\gamma = 775$ MeV, which accounts for the ρ^- meson. The dashed curve in Fig. 1(b) represents the sum of 50% invariant phase space and 50% invariant phase space with a normalized Breit-Wigner resonance term of the form $N/[(\omega - \omega_\gamma)^2 + (\frac{1}{2}\Gamma)^2]$. The resonance term used has a value of full width at half-maximum $\Gamma = 125$ MeV. This curve is normalized to the ρ^- peak. The (π^-, π^+) spectrum is also strongly peaked at a central value of $\omega_\gamma = 775$ MeV, which accounts for the ρ^0 meson; however, here the resonance width appears to be broader than the width of the ρ^- meson. With the mixture of invariant phase space and phase space with resonance, determined by the ρ^- spectrum, the dashed curve in Fig. 1(a) is computed by using a value of $\Gamma = 175$ MeV. This curve fits best around the ρ^0 region and is normalized to the ρ^0 peak.

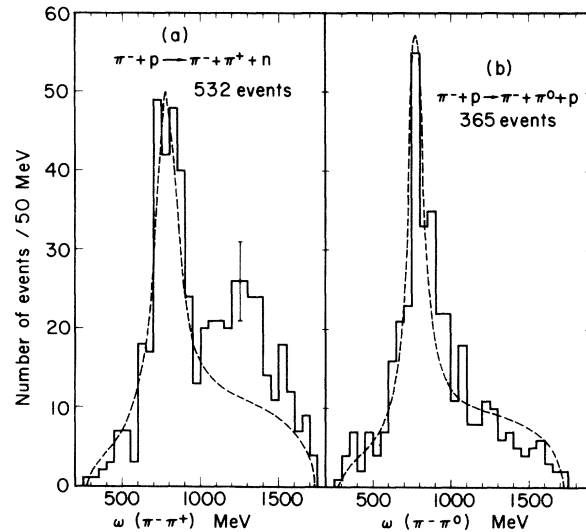


FIG. 1. (a) Spectrum of $\omega(\pi^-, \pi^+)$ from 532 events of reaction $\pi^- + p \rightarrow \pi^- + \pi^+ + n$. Dashed curve: 50% invariant phase space and 50% invariant phase space with Breit-Wigner resonant term using $\Gamma_\gamma = 175$ MeV, $\omega_\gamma = 775$ MeV. (b) Spectrum of $\omega(\pi^-, \pi^0)$ from 365 events of reaction $\pi^- + p \rightarrow \pi^- + \pi^0 + p$. Dashed curve: same as in (a) with $\Gamma_\gamma = 125$ MeV, $\omega_\gamma = 775$ MeV.

A second peak in the (π^-, π^+) spectrum is observed with a central value $\omega_\gamma = 1250$ MeV and a width of $\Gamma \approx 200$ MeV. Similar peaks have been seen in two recent experiments.¹⁻³ The shoulder seen around 1050 MeV which appeared to be resolved at an earlier stage of this experiment has lost its resolution in this final analysis.

To study the resonant behavior of these peaks we have constructed distributions in $\cos\theta_{\pi\pi}$ for several segments of the ω spectrum. Due to the ω^2/μ^2 vs Δ^2/μ^2 phase-space limitations, the angular distributions are presented with lower limits of t chosen as $t_{\min} \approx 0$ for $275 < \omega < 1000$ MeV, and $t_{\min} = 4.0 \mu^2$ for $1000 < \omega < 1450$ MeV. Distributions were made in t for various segments of ω in both reactions. All of these distributions showed a characteristic dependence $t/(t+1)^2$. Most of the events were confined to values below $t = 25 \mu^2$, the rest being dispersed in a tail extending to $t_{\max} = 275 \mu^2$. Accordingly, the angular distributions are presented with the upper limit of $t = 20 \mu^2$. Figure 2(a) is the angular distribution at the ρ^- resonance showing a characteristic $\cos^2\theta$ dependence over a constant background, $700 \leq \omega(\pi^-, \pi^0) < 850$ MeV. Figure 2(b) is the angular distribution above the ρ^- resonance, $850 \leq \omega(\pi^-, \pi^0) < 1000$ MeV. The forward peak indicates that the p -wave shift, δ_1 , has crossed over 90° . Figure 2(c) shows that the angular distribution at the ρ^0 resonance is strongly peaked in the forward direction, $700 \leq \omega(\pi^-, \pi^+) < 850$ MeV. This behavior continues after the ρ^0 resonance as seen in Fig. 2(d), $850 \leq \omega(\pi^-, \pi^+) < 1000$ MeV. This indicates that an s -wave or a d -wave phase shift from the isotopic spin $T=0$ component of the (π^-, π^+) state is sufficiently strong to interfere with the p -wave phase shift of the $T=1$ component δ_1 , such that it prevents the effective phase shift from reaching 90° at the ρ^0 resonance. The $T=2$ component is ruled out for such a behavior since it would have appeared in both reactions.

Figures 2(e), 2(f), and 2(g) show the angular distribution before the peak [$1000 \leq \omega(\pi^-, \pi^+) < 1150$ MeV], at the 1250-MeV peak [$1150 \leq \omega(\pi^-, \pi^+) < 1300$ MeV], and after the peak [$1300 \leq \omega(\pi^-, \pi^+) < 1450$ MeV], respectively; Fig. 2(f) is a non-isotropic symmetric distribution. The 1250-MeV peak is seen in the (π^-, π^+) state and not in the (π^-, π^0) , so that this resonance has isotopic spin $T=0$; whereby, it is confined to even angular momenta. Although Fig. 2(f) does not show the characteristic d -wave hump at $\theta_{\pi\pi} = 90^\circ$, the $J=0$ value is ruled out by nonisotropy. Dalitz

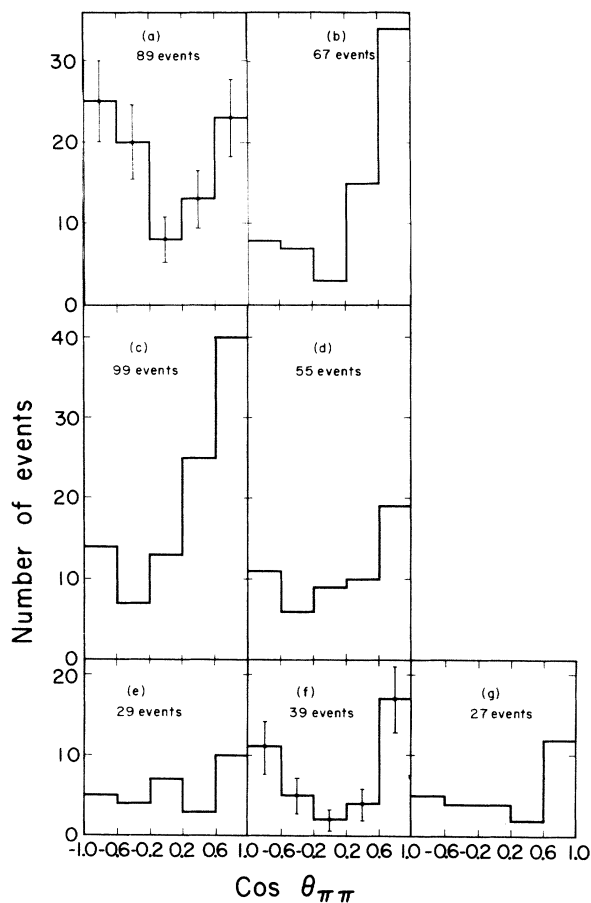


FIG. 2. Distributions in $\cos\theta_{\pi\pi}$, the angle between the incoming and outgoing π^- in the barycentric system of the final pions. (a) $700 \leq \omega(\pi^-, \pi^0) < 850$ MeV, and $t_{\min} < t \leq 20 \mu^2$; (b) $850 \leq \omega(\pi^-, \pi^0) < 1000$ MeV, and $t_{\min} < t \leq 20 \mu^2$; (c) $700 \leq \omega(\pi^-, \pi^+) < 850$ MeV, and $t_{\min} < t \leq 20 \mu^2$; (d) $850 \leq \omega(\pi^-, \pi^+) < 1000$ MeV, and $t_{\min} < t \leq 20 \mu^2$; (e) $1000 \leq \omega(\pi^-, \pi^+) < 1150$ MeV, and $4.0 \mu^2 < t < 20 \mu^2$; (f) $1150 \leq \omega(\pi^-, \pi^+) < 1300$ MeV, and $4.0 \mu^2 < t \leq 20 \mu^2$; and (g) $1300 \leq \omega(\pi^-, \pi^+) < 1450$ MeV, and $4.0 \mu^2 < t \leq 20 \mu^2$.

plots were constructed for Reactions (a) and (b). Figure 3 represents the projections of those plots in terms of the final pion reaction center-of-mass kinetic energies, T_π . The curves shown are the invariant phase-space integrals normalized to the total area of each histogram. The position of possible pion-nucleon resonances are indicated accordingly. Figures 3(a₁) and 3(a₂) are the T_{π^+} and T_{π^-} projections, which are equivalent to the (π^-, n) and (π^+, n) effective-mass spectra, respectively. No appreciable deviation from phase space is seen in either state. Figures 3(b₁) and 3(b₂) are the T_{π^0} and T_{π^-} projections, giving the (π^-, p) and (π^0, p) effective-mass spectra, respectively. Deviations from phase space are evident

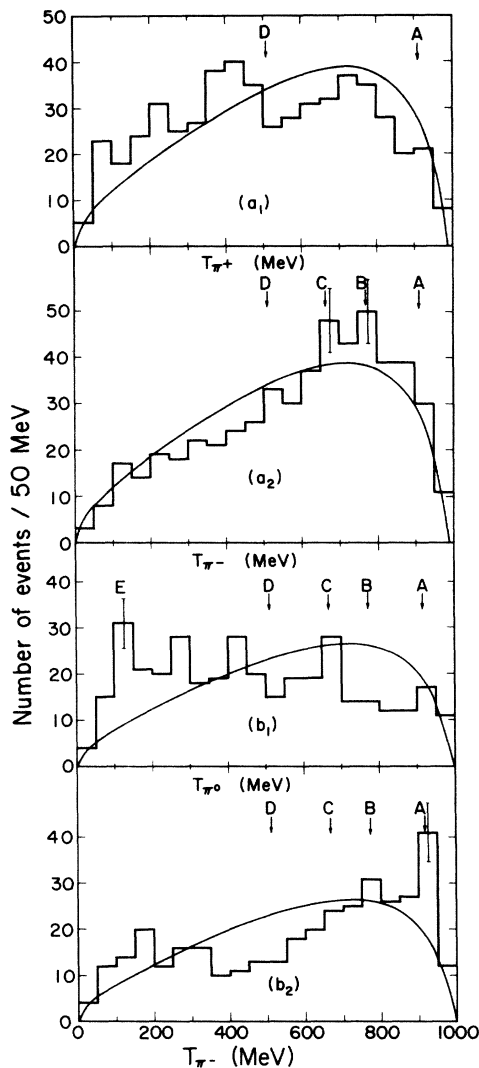


FIG. 3. Projections of Dalitz plots in terms of final pion c.m. kinetic energies. (a₁) and (a₂) are projections from $\pi^- + p \rightarrow \pi^- + \pi^+ + n$; (b₁) and (b₂) are from $\pi^- + p \rightarrow \pi^- + \pi^0 + p$. Solid curves are phase-space integrals. Positions of possible N^* resonances are indicated by A, B, C, and D for the pion-nucleon effective-mass values of 1238, 1512, 1688, and 1920 MeV, respectively; E has the value of 2400 MeV.

in both states. The T_{π^0} distribution has a 4-standard-deviation peak corresponding to 2400-MeV (π^-, p) effective mass. The T_{π^-} distribution has a 3.5-standard-deviation peak at the $N_{3/2}^*(1238)$ position. If the peak in the T_{π^-} distribution is assumed to be due to the $N_{3/2}^*(1238)$ resonance, then the 2400-MeV peak in the T_{π^0} distribution must be considered as spurious. An examination of the Dalitz plot of Reaction (b) shows that 40% of the events at the 2400-MeV

region of T_{π^0} come from the $N_{3/2}^*(1238)$ of T_{π^-} , and 25% from the ρ^- resonance.

In Reaction (a) the final state $\pi-\pi$ resonances dominate over (π, n) interactions, whereas in Reaction (b), with the presence of a single $\pi-\pi$ resonance, the remaining phase space is available to the pions for any (π, p) interactions.

Conclusion. — The striking difference in the angular distribution between the ρ^0 and the ρ^- needs further explanation. This difference seems to be independent of energy.⁴ If the apparent enlargement of the ρ^0 width is due to an adjacent ω^0 which decays electromagnetically⁵ into two pions, then interference with this same process cannot explain the forward asymmetry in the ρ^0 decay angular distribution. This is because the general form for the angular distribution of a vector particle decaying into two pions, when averaged over the azimuthal angle ϕ , is of the form⁶ $a + b \cos^2 \theta_{\pi\pi}$ whether the mechanism is strong or electromagnetic. The azimuthal angle ϕ is measured with respect to the normal to the ρ^0 or ω^0 production plane.

Recent experiments on high-energy $p-p$ elastic scattering indicate that the first Pomernanchuk trajectory may have a slope⁷ of $\alpha_{P_1}'(0) \approx 1/80 \mu^2$. If the Regge singularities are confined to simple poles and if a constant slope of Regge trajectories is assumed⁸ over a wide energy range, then the 1250-MeV $T=0$ $\pi-\pi$ resonance can be interpreted as the physical manifestation of P_1 . Recently, a second Pomernanchuk trajectory P_2 , with the intercept value⁹ $\alpha_{P_2}(0) \approx 0.5$, has been postulated.⁹⁻¹² Under the above assumptions this should manifest itself as a $T=0$ $\pi-\pi$ resonance at 1800 MeV, which is above the phase-space limitations of this experiment.

I am grateful to Professor Wilson M. Powell for his support and encouragement and to Dr. Robert W. Birge for numerous discussions and guidance. This experiment would not have been possible without the efforts of many in the Powell-Birge research group. I would like to thank Professor Luis W. Alvarez and his group for the bubble chamber exposure, and the data analysis group of Howard White for the data reduction.

*Work done under the auspices of the U. S. Atomic Energy Commission.

†Present address: Stanford Linear Accelerator Center, Stanford University, Stanford, California.

¹J. Hennessy, J. J. Veillet, M. di Corato, and P. Negri, Proceedings of the International Conference

on High-Energy Nuclear Physics, Geneva, 1962, reported by F. Muller (CERN Scientific Information Service, Geneva, Switzerland, 1962).

²W. Selove, N. Hagopian, H. Brody, A. Baker, and E. Leboy, *Phys. Rev. Letters* **9**, 272 (1962).

³J. J. Veillet, J. Hennessy, H. Bingham, M. Bloch, D. Drijard, A. Lagarrigue, P. Mittner, A. Rousset, G. Bellini, M. di Corato, E. Fiorini, and P. Negri, *Phys. Rev. Letters* **10**, 29 (1963).

⁴For a discussion on the ρ width at a lower energy, see Saclay-Orsay-Bari-Bologna collaboration (to be published).

⁵J. Bernstein and G. Feinberg, Proceedings of the International Conference on High-Energy Nuclear Physics, Geneva, 1962 (CERN Scientific Information Service, Geneva, Switzerland, 1962).

⁶S. M. Berman, Stanford Linear Accelerator Center, Stanford University, Stanford, California (private communication).

⁷K. J. Foley, S. J. Lindenbaum, W. A. Love, S. Ozaki, J. J. Russell, and L. C. L. Yuan, Brookhaven National Laboratory preprint, 1963 (unpublished).

⁸G. F. Chew and S. C. Frautschi, *Phys. Rev. Letters* **8**, 41 (1962).

⁹K. Igi, *Phys. Rev. Letters* **130**, 820 (1963).

¹⁰K. Igi, *Phys. Rev. Letters* **9**, 76 (1962).

¹¹S. D. Drell, Proceedings of the International Conference on High-Energy Nuclear Physics, Geneva, 1962 (CERN Scientific Information Service, Geneva, Switzerland, 1962).

¹²F. Hadjioannou, R. J. N. Phillips, and W. Rarita, *Phys. Rev. Letters* **9**, 183 (1962).

ρ -MESON REGGE TRAJECTORY AND HIGH-ENERGY CHARGE-EXCHANGE SCATTERING

Ivan J. Muzinich

University of Washington, Seattle, Washington

(Received 27 May 1963)

The n - p charge-exchange differential and total cross sections were recently measured at 2.04 and 2.85 BeV.¹ A very sharp forward peak was reported in the differential cross section. A possible explanation of this sharp peak was proposed by Phillips² in terms of an interference between the single pion contribution and the background part of the NN amplitude. The purpose of this communication is to propose an alternative explanation in terms of the ρ meson treated as a Regge pole. If this explanation is indeed correct, the high-energy π^- - p and K^- - p charge-exchange reactions should also show a similar sharp peak for small momentum transfers.

It is well known that only the exchange of particles and resonances of isospin 1 or greater are possible for charge exchange. Of the known particles and resonances, the ρ and π mesons should be important for n - p charge exchange and the ρ meson only for π^- - p and K^- - p charge exchange. In the n - p case if the π and ρ mesons are treated as poles in lowest order perturbation theory with currently expected coupling constants³ $g_{\rho \rightarrow N\bar{N}}^2/4\pi \approx 2$ and $g_{\pi \rightarrow N\bar{N}}^2/4\pi = 15$, one finds total disagreement with the experimental results in reference 1. This is not surprising since the ρ contribution, due to the large ρ mass, gives rise to a broad peak, and the π contribution which is 0 in the forward direction is too large at the larger angles. Because of the spin structure of the NN amplitude and the quantum numbers of the π and ρ mesons, an interference between the π and ρ contributions

is impossible and any one-pion contribution is additive.

In this communication the ρ -meson Regge trajectory is assumed to be the dominant mechanism in high-energy charge exchange, and it is shown that the slope of the ρ trajectory $\alpha'(t)$, $t \leq 0$, can be adjusted to give rough agreement with the n - p experimental data¹ for small momentum transfers. The ρ meson treated as a Regge pole gives a different angular distribution than the broad angular distribution from that due to the ρ treated as a perturbation-theory pole.

A detailed treatment of the NN problem in terms of Regge poles is given.⁴ The contribution of the ρ trajectory to the NN helicity-nonflip amplitude is

$$\phi^T(s, t) = -\frac{\pi}{2(s)^{1/2}} \frac{\beta(t)}{\sin \pi \alpha(t)} [2\alpha(t) + 1] \times [\mathcal{O}_{\alpha}(-z_t) - \mathcal{O}_{\alpha}(z_t)]^{\frac{1}{2}} [1 + 2(-1)^T], \quad (1)$$

where $\beta(t)$ and $\alpha(t)$ are the residue and position of the ρ trajectory. The quantities s and t are the usual Mandelstam variables. The ρ is exchanged in the t $N\bar{N}$ channel. The quantity T is the total isospin for the NN channel. The function $\mathcal{O}_{\alpha}(z_t)$ is related to the hypergeometric function⁵ by

$$\mathcal{O}_{\alpha}(z_t) = \frac{(2z_t)^{\alpha} \Gamma(\alpha + \frac{1}{2})}{\Gamma(\alpha + 1)(\pi)^{1/2}} F\left(\frac{1}{2}(1 - \alpha), -\frac{1}{2}\alpha, \frac{1}{2} - \alpha, \frac{1}{z_t}\right), \quad (2)$$